Research Article

Rakesh Goswami*, Anita Khosla, Aftab Alam and Pradeep K. Varshney

Experimental investigation on the spectral, mechanical, and thermal behaviors of thermoplastic starch and de-laminated talc-filled sustainable bio-nanocomposite of polypropylene

https://doi.org/10.1515/jmbm-2024-0031
received August 26, 2024; accepted December 21, 2024

Abstract: This study delves into sustainable bio-nanocomposite of polypropylene (PP) with thermoplastic starch and de-laminated nano-talc as filler. Synthesis and characterization were done in two stages, at first, thermoplastic starch in the PP matrix was kept at 15, 20, and 25% and bio-composite was investigated for their spectral, optical, mechanical, and thermal properties. Results revealed enhanced tensile strength, elongation, flexural strength, melt flow index, and melting point of the composite with 20% starch compared to other formulations. Thereafter, the PP matrix with 20% starch was taken as the base polymer, the concentration of nano-talc was kept at 1, 3, and 5%, and investigation of their mechanical properties revealed composite with 20% starch and 3% nano-talc to be better than those with 20% starch and nano-talc of 1 or 5%. Integration of 3% talc filling into the bio-composite material increased the tensile strength to 29.27 MPa and flexural modulus to 2964.6 MPa but, with marginal reduction in elongation and flexural strength to 1.03% and 40.59 Mpa, respectively. Increased mechanical properties can be attributed to the action of glycerol as a plasticizer and the uniform dispersion of fillers. X-ray diffraction study revealed uniform interplanar arrangement and crystal size whereas UV-Visio studies showed a decrease in ultraviolet absorbance. Differential scanning calorimetry and thermogravitational analysis studies revealed improved thermal stability.

Keywords: bio-composite, mechanical properties, nano-talc, polypropylene, starch, UV absorbance

*** Corresponding author: Rakesh Goswami,** Department of Electrical and Electronics Engineering, SET, Manav Rachna International Institute of Research and Studies, Faridabad, Haryana, 121004, India, e-mail: rakesh.goswami@dseu.ac.in
Anita Khosla: Department of Electrical and Electronics Engineering, SET, Manav Rachna International Institute of Research and Studies, Faridabad, Haryana, 121004, India, e-mail: anitakhosla.set@mriu.edu.in
Aftab Alam: Department of Polymer Technology, Guru Nanak Dev DSEU Rohini Campus, Sector 15, Rohini, Delhi, 110089, India, e-mail: aftab.alam@dseu.ac.in
Pradeep K. Varshney: Department of Academic Processes and Quality Assurance, Swami Rama Himalayan University, Jolly Grant, Dehradun, Uttarakhand, 248016, India, e-mail: varshney70@rediffmail.com

1 Introduction

Polypropylene (PP), a synthetic polymer and second most widely used [1] thermoplastic material, is one of the most popular choices for common industrial and household applications, *i.e.*, electrical insulation, electrical and electronic component housing, beverage packaging, food industry, agricultural applications, automobile components, civil construction materials, *etc.* [2,3]. Despite huge worldwide plastic consumption, only 10% of the total disposed of plastic material stands recycled and the rest ends up either in landfill or is left in the environment as pollutant [4]. Global plastic pollution has come to an extent, causing significant ecological imbalance and global climate threat. Green theory [5] evolved during these days and has brought the attention of researchers toward the development of materials from environment-friendly sources, produced with minimal environmental impact and offering benefits throughout the product life cycle. In the quest for sustainable and renewable plastic material, several researchers incorporated several bio-fillers [6–10] in the PP matrix for bio-degradability and cost reduction. Starch being one such naturally available thermoplastic polymer became popular [3,6,11,12] to the extent that 1% of the total global plastic production now contains starch [13]. Thermoplastic starch, which has been certified for its sustainability and biodegradability by several prominent organizations such as International Sustainability and Carbon Certification, Roundtable on Sustainable Biomaterials, Global Bioenergy Sustainability Framework, and USDA BioPreferred, exhibits all the characteristics of green futuristic material, *i.e.*,

source, production, and life cycle. Therefore, blending thermoplastic starch with a conventional polymeric material such as PP offers ecologically sustainable bio-materials, but such materials find limited industrial application because of the hydrophobic nature of PP which is just opposite to that of hydrophilic starch. Several researchers investigated the hydrophobicity [14,15], bio-degradability [14,16], morphology [17] crystallinity [3], dielectric strength [18], and thermal and mechanical properties [14,15,19] of starch-based PP bio-composite. Results therein indicated a reduction in mechanical [20–22], thermal, and electrical performance [23] attributable to the poor diffusion of starch molecules in the polymeric matrix and poor bond of filler molecules with a polymer matrix [24,25]. Talc, another low-cost natural filler is a magnesium silicate-based geo-material that has also been found readily compatible with the PP matrix [26], this mineral material has been found to enhance the mechanical, thermal, and electrical properties of thermoplastic polymer in several studies [27–29]. It was found that talc as filler in the PP matrix increases the tensile strength and flexural strength but simultaneously reduces the impact strength [30–34] of composite materials. To address such issues and several other challenges like scalability and cost-effectiveness in developing sustainable engineering material, and keeping in view the bio-degradable nature of starch, this study delves into the synthesis and characterization of starch-based bio-composite of PP. To cater to the starch-induced decrease in mechanical properties, de-laminated nano-talc was also incorporated as another natural filler. Bio-nanocomposites were characterized for the effects of starch and nano-talc on their mechanical, thermal, and ultraviolet (UV) absorbance properties.

2 Materials and preparation

PP (homo-polymer) of grade PPH350FG was procured from Reliance Industries (India) as a base polymer matrix. Potato starch (MW 162.14) was obtained from Loba Chemie (Mumbai), de-laminated nano-talc from Golcha Group (Rajasthan, India), and glycerol (99.5%) from M/s Fisher Scientific (Mumbai, India). The bio-nanocomposites were prepared by homogeneously mixing starch with glycerol and left over for a night hours to swell. The thermoplastic starch and PP were then mixed in an ultrahigh-speed mixer until they turned into molten form. Finally, molten material was molded into a test specimen by compression molding techniques, and specimens were prepared as per applicable ISO/ASTM standards. The formulation of PP bio-nanocomposite is given in Table 1.

Table 1: Formulation of starch and nano-talc-filled PP bio-composite

Sample name	PP (% volume)	Thermoplastic starch (%)	De-laminated nano-talc (%)
Pure PP	100	0	0
PPST-15	85	15	0
PPST-20	80	20	0
PPST-25	75	25	0
PPSTTL 2001	79	20	1
PPSTTL 2003	77	20	3
PPSTTL 2005	75	20	5

3 Characterization

3.1 Spectral characterization

The plastic identification test was done by Fourier transform infrared (FTIR) spectroscopy as per test standard ASTM E 1252-98 (Ra 2021), samples were scanned in the wavelength range 400–4,000 cm^{-1}, and the spectrum was evaluated to obtain stretching/bending vibrations for identification of the molecular structure of the composite materials.

Bio-nanocomposite specimens were also subjected to an X-ray diffraction (XRD) pattern, and the intensity of X-rays diffracted by the specimen in 2θ range 5° to 80° was recorded to assess its atomic orientation/structure, crystallinity, and phase purity. XRD spectrum gave insight into the crystallinity and molecular orientation of bio-nanocomposite material.

UV-Visio range UV–visible [UV–Vis] spectrophotometry of the samples was also done to obtain their UV–Vis range optical absorbance, and specimens were scanned in the wavelength 200–800 nm for absorbance spectrum.

3.2 Thermal characterization

Differential scanning calorimetry (DSC) test has been done as per standard ISO 11357-1:2023. The thermal behavior of the bio-nanocomposite was obtained as a thermogram which provided insight into its melting and crystallization behavior. Thermogravitational analysis (TGA) was also done to examine the pattern of thermal degradation; results indicated the temperature range within which

bio-nanocomposite shall remain stable. Test has been done as per ASTM 1131:2000 test standards to ascertain its decomposition behavior, thus indicating its reliability for optimum performance.

3.3 Mechanical characterization

Mechanical characterization of bio-nanocomposite was done by measurement of its tensile strength, elongation, flexural properties, and melt flow index (MFI). Tensile strength and elongation tests were done following ISO 527-1:2019 standards, whereas measurements of flexural properties and MFI were done following ISO 178:2019 and ISO 1133-1:2022 (procedure B), respectively.

4 Results and discussion

4.1 FTIR spectroscopy

Figure 1(a) depicts the FTIR spectra of PP, PPST-15, 20, and 25, this spectrum helps identify the presence of PP and thermoplastic starch in the bio-composite. Absorbance peaks near 972.261 and 1168.149 cm^{-1} may be attributed to the stretching vibration because of C–C bond, which is the backbone of the PP matrix. C–H bond in the CH_3 (methyl group) and CH_2 (methylene group) can be attributable to the C–H stretching vibration linked to an absorbance peak between 2865.123 and 2993.56 cm^{-1}.

Absorbance peaks around 1455.88 and 1376.234 cm^{-1} can also be attributed to the bending vibration due to the

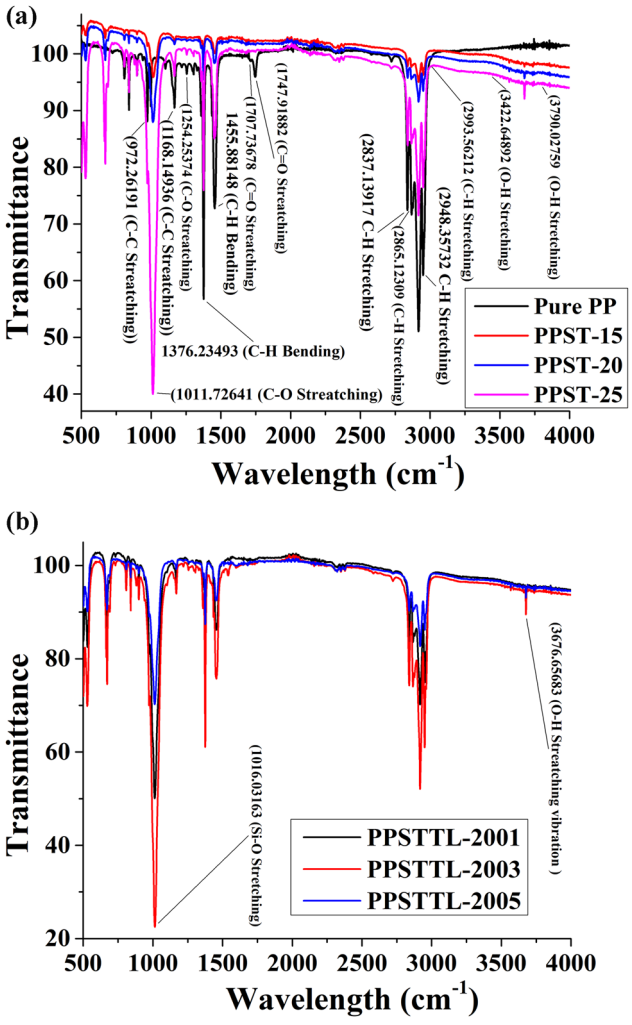

Figure 1: (a) FTIR spectrum of PP, PPST-15, 20, and 25. (b) FTIR spectrum of PPSTTL 2001, 2003, and 2005.

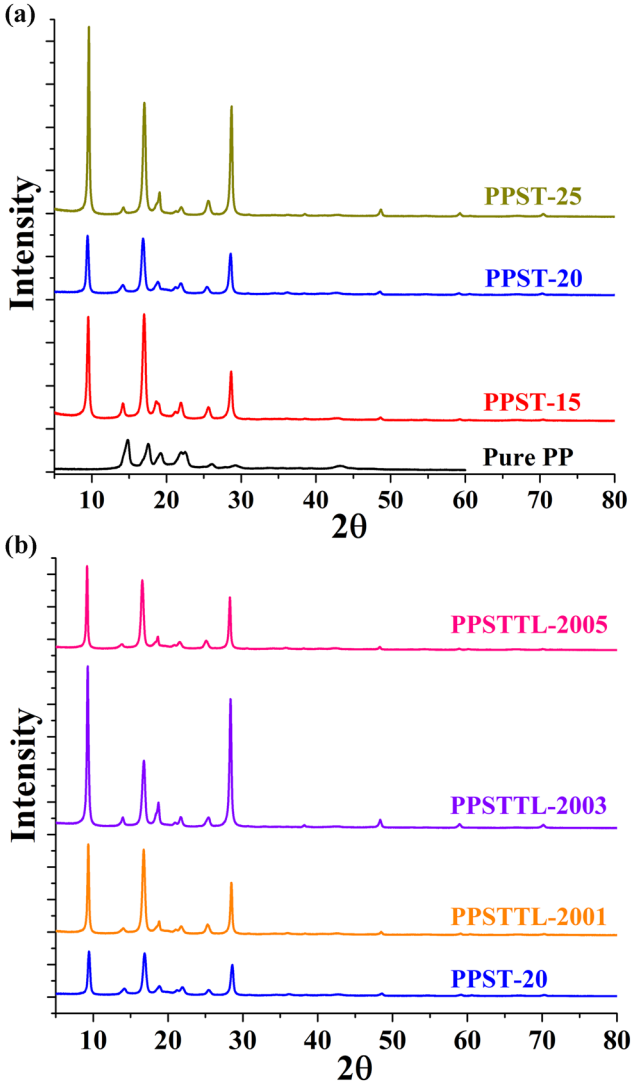

Figure 2: (a) XRD spectrum of Pure PP, PPST-15, 20, and 25. (b) XRD spectrum of PPSTTL 2001, 2003, and 2005.

C–H bond of the PP matrix [35–37]. Absorbance peak around 3422.648 to 3790.027 cm^{-1} indicates O–H stretching vibration; this can be attributable to the hydroxyl group associated with thermoplastic starch molecule [35–37], and another absorbance peak around 2837.139–2948.357 cm^{-1} indicates stretching vibration due to its C–H bond. The carbonyl group and glycosidic bond are starch components, for which, C═O stretching vibration at 1707.736 to 1747.918 cm^{-1} indicates carbonyl group and C–O stretching vibration at 1011.726–1254.253 cm^{-1} indicates glycosidic bond. Upon successful verification of the presence of PP matrix and starch as filler, let us consider Figure 1(b) which depicts the FTIR spectra of bio-nanocomposite PPSTTL 2001, 2003, and 2005; this contains PP as a base matrix, 20% thermoplastic starch as bio-filler, and de-laminated talc as nano-filler in concentration 1, 3, and 5%.

From the FTIR spectra shown in Figure 1(b), it looks like that all the absorbance peaks for PP and thermoplastic starch, which were indicated in Figure 1(a), are present in Figure 1(b) as well; those absorbance peaks are indicative of the presence of PP and starch in the bio-nanocomposite. In addition to all the absorbance peaks marked in Figure 1(a),

Table 2: XRD data of bio-nanocomposite

Sample	2θ	$\beta \cos \theta$	FWHP (θ)	FWHP (Rd)	Crystal size (nm)	*d*-spacing (A°)
PP	14.7	0.015986	0.92349	0.016118	8.673509	6.018909477
	17.4551	0.017383	1.00765	0.017587	7.976127	5.074599634
	19.161	0.017636	1.02476	0.017885	7.861791	4.626472208
	21.966	0.022871	1.33489	0.023298	6.06215	4.041620362
	22.5867	0.007851	0.4587	0.008006	17.66064	3.93194366
	26.0744	0.011965	0.70367	0.012281	11.5882	3.413373412
	29.2009	0.021235	1.2573	0.021944	6.529213	3.054627817
	43.2354	0.027611	1.70169	0.0297	5.021551	2.09005269
PPST-15	9.4983	0.007361	0.42321	0.007386	18.83569	9.300255632
	14.1616	0.010041	0.5797	0.010118	13.8091	6.246513564
	16.988	0.009176	0.53157	0.009278	15.11031	5.213063991
	18.6995	0.018583	1.07906	0.018833	7.461161	4.739616842
	21.8461	0.014618	0.853	0.014888	9.484953	4.06352526
	25.5956	0.009529	0.55986	0.009771	14.55088	3.476129827
	28.6226	0.007756	0.45864	0.008005	17.87569	3.115015502
PPST-20	9.43393	0.00722	0.41511	0.007245	19.20233	9.363568638
	14.14566	0.01684	0.97224	0.016969	8.233561	6.253507794
	16.86148	0.009578	0.55478	0.009683	14.47577	5.25189428
	18.80425	0.016763	0.97353	0.016991	8.271194	4.713442517
	21.73178	0.017398	1.01505	0.017716	7.969175	4.084646213
	25.43456	0.010231	0.60093	0.010488	13.55211	3.497767651
	28.55698	0.007855	0.46441	0.008105	17.65102	3.1220198
PPST-25	9.58069	0.005918	0.34028	0.005939	23.42756	9.220461297
	14.22654	0.008892	0.5134	0.008961	15.5935	6.218136961
	17.02487	0.008658	0.50157	0.008754	16.01486	5.20185721
	18.92364	0.013305	0.77281	0.013488	10.42125	4.683973484
	21.92144	0.011317	0.66044	0.011527	12.25197	4.049733227
	25.59312	0.009383	0.55131	0.009622	14.77647	3.476455705
	28.67496	0.006682	0.39513	0.006896	20.75131	3.109442177
PPSTTL 2001	42.549	0.018694	1.1494	0.020061	0.021487	2.122167757
	48.46658	0.006573	0.41298	0.007208	0.002714	1.8759764
	54.50358	0.019227	1.2392	0.021628	0.023827	1.681583664
	59.05988	0.008377	0.55162	0.009628	0.004621	1.562251781
PPSTTL 2003	42.305	0.029209	1.79445	0.031319	0.052414	2.133841641
	48.3441	0.006963	0.43731	0.007632	0.003045	1.880442744
	54.47221	0.01139	0.73397	0.01281	0.00836	1.682477943
	58.95131	0.007626	0.50192	0.00876	0.003828	1.564869847
PPSTTL 2005	42.346	0.024758	1.52122	0.02655	0.037662	2.1318704
	48.276	0.006083	0.38193	0.006666	0.002323	1.882936217
	54.32763	0.017233	1.10976	0.019369	0.019124	1.68661351
	58.89365	0.007168	0.4716	0.008231	0.00338	1.566264408

spectrum at Figure 1(b) contains a sharp and strong absorbance peak at 1016.031 cm^{-1} corresponding to the stretching vibration of the Si–O bond and a peak at 3676.656 cm^{-1} corresponding to the stretching vibration because of O–H without hydrogen bond; both these peaks are indicative of the successful presence of talc as nano-filler [38–40] in all the bio-nanocomposite.

4.2 XRD

Figure 2(a) and (b) depict the XRD spectra of PP, PPST-15, 20, and 25 and PPSTTL 2001, 2003, and 2005, respectively, both spectra form the basis to identify the crystallinity and atomic structure of bio-nanocomposite.

Diffracted X-rays were analyzed in 2θ range 5–80° for the phases plane, crystal size, and interplanar spacing. Interplanar spacing was calculated by applying the following equation and the same is presented in Table 2.

From the Braggs law, we know that

$$n\lambda = 2 \times d \times \sin\theta, \quad (1)$$

where n is the order of reflection, λ is the X-ray wavelength, d is the interplanar spacing, and θ is the angle of diffraction.

XRD peaks and corresponding 2θ values of pure PP, PPST-15, 20, and 25 were found to be around 14–16°, 21–23°, and 29–31° which corresponds to the interplanar spacing along (110) plane, (200) plane, and (040) plane, respectively. Larger d-spacing found in all these bio-composites compared to the pure PP suggests less dense packing of starch molecules within the crystalline structure. Furthermore, the smaller interplanar spacing in the bio-nanocomposite PPSTTL 2001, 2003, and 2005 indicates the more orderly distribution of starch and delaminated nano-talc molecules within the crystalline structure of the PP matrix; this can also be verified from the crystal size of the starch-based composite and delaminated nano-talc-filled bio-nanocomposite in Table 2. The relative decrease in XRD peaks of the bio-nanocomposite indicates that some nanoparticles may have been exfoliated. Even though FTIR and XRD spectral measurement methods are volume dependent, *i.e.*, the intensity of a given peak of a substance is proportional to the volume fraction of the substance in the sample, still, comparison of the subtracted graph is not common in XRD analysis, which is in contrast to FTIR analysis. Results indicate that the intensity of diffraction peak at 90 due to nano-talc is highest for PPSTTL 2003 (*i.e.*, with 3% loading) in Figure 2(b). This indicates the highest level of dispersion with a 3% loading of nano-talc in bio-composites with 20% thermoplastic starch. The same was also confirmed by improved thermal and mechanical properties of PPSTTL 2003 bio-nanocomposites.

4.3 UV–Vis spectrophotometry

Pure PP and its bio-composites, *i.e.*, PPST-15, 20, and 25, were subjected to UV-Viso spectrophotometry, and the absorbance spectrum is presented in Figure 3(a) for analysis.

The absorbance spectrum was analyzed in the UV short wave range 200–280 nm, middle wave range 280–315 nm, and long wave range 315–400 nm for the effect of increasing thermoplastic starch content on the UV absorption property of the bio-composites. Thermoplastic starch is known to be hydrophilic and possesses photosensitizer properties [37]; both this property causes the starch molecules to absorb energy possessed by UV lights in all three UV ranges, and this energy ultimately gets transferred to the PP matrix. UV range absorbance spectrum for PPST-15, 20, and 25 is shown in Figure 3(a) indicating its increasing absorbance of UV

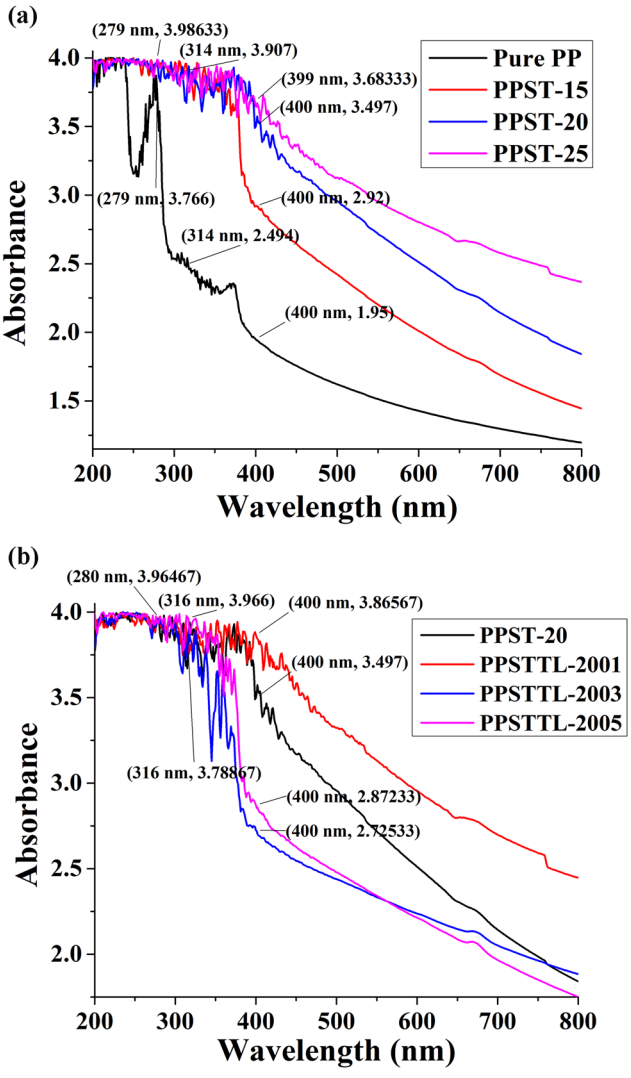

Figure 3: (a) UV-Visio absorbance spectrum of Pure PP, PPST-15, 20, and 25. (b) UV-Visio absorbance spectrum of PPSTTL 2001, 2003, and 2005.

light in all three UV ranges; this can directly be linked to the increasing concentration of the starch in the PP matrix [37]. Increased absorption of UV energy by all the bio-composite may result in breakage of the chemical bonds of the PP matrix and, thus, faster degradation of the material upon UV exposure. To compensate for the increasing absorption of UV energy by the bio-composite, delaminated nano-talc was included as filler in the bio-composite of PP and starch. PP composite having 20% starch concentration exhibited better mechanical and thermal properties than other bio-composites having 15 and 25% starch filler; thus, nano-talc was infused into it at concentrations of 1% (PPSTTL 2001), 3% (PPSTTL 2003), and 5% (PPSTTL 2005), and the specimen was subjected to UV–Vis spectrophotometry; thermal and mechanical studies of the bio-nanocomposite have also been done in the later part of this study and not included in this section. UV-Visio absorbance spectra of PPST-20, PPSTTL 2001, 2003, and 2005 are presented in Figure 3(b).

Figure 3(b) reveals increased UV absorbance of PPSTTL 2001 when compared to that of PPST-20, whereas the same was found to decrease for the PPSTTL 2003 and PPSTTL 2005; the lowest absorbance in the entire UV range was found to be of PPSTTL 2003 which contained 3% talc filler. Talc is characterized by its property to take part in absorbing some UV radiation and, simultaneously, is also characterized to act as a nucleating agent when used below 3% concentrations and act as a reinforcement filler when used at higher concentrations [26]. From Figure 3(b), it can be inferred that bio-nanocomposite with delaminated nano-talc concentration of 3% acted as a nucleating agent for both starch molecules and polymer matrix, thus reducing the amount of UV radiation penetrated in the PP matrix, hence slowing down the UV induced degradation process [26,41,42]. Large crystals scatter incident lights in a way different from that of smaller crystal size, thus influencing their optical behavior. In this study, small crystal size and smaller

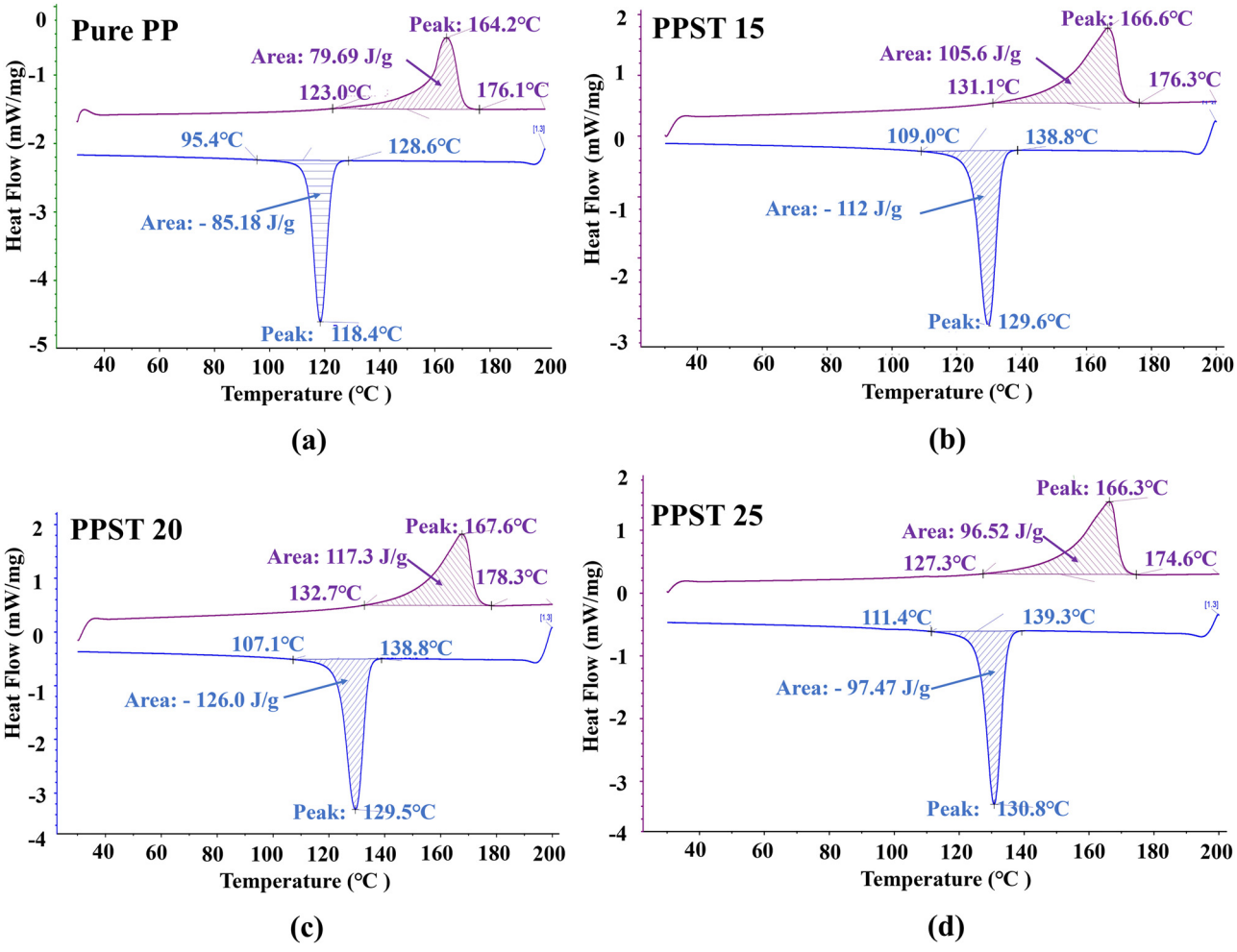

Figure 4: DSC thermogram of (a) pure PP, (b) PPST-15, (c) PPST-20, and (d) PPST-25.

Table 3: DSC detailed data of the pure PP, PPST-15, 20, and 25

Samples	Melting temperature T_m (°C)	Enthalpy change (melting) ΔH_m (J/g)	Crystallization temperature T_c (°C)	Enthalpy change (cooling) ΔH_c (J/g)	Degree of crystallinity X_c (%)
Pure PP	164.2	79.69	118.4	85.18	44.83
PPST-15	166.6	105.6	129.6	112	58.95
PPST-20	167.6	117.3	129.5	126	66.32
PPST-25	166.3	96.52	130.8	97.47	51.3

interplanar spacing (*d*-spacing) within the crystal structure of bio-nanocomposite PPSTTL 2001, 2003, and 2005 when compared to that of PPST-15, 20, and 15 indicated more uniformly and orderly distribution of delaminated nano-talc molecules within the PP matrix. High orientation in the crystal chain of the bio-nanocomposite may have led to the birefringence of incident light and, thus, an obvious reduction in its UV absorbance.

4.4 DSC studies

DSC thermogram in Figure 4(a)–(d) represents the thermal behavior of pure PP, PPST-15, 20, and 25, respectively; this curve indicates their melting and crystallization phases during the heating and cooling cycle, respectively. The results extracted from the thermogram are summarized in Table 3.

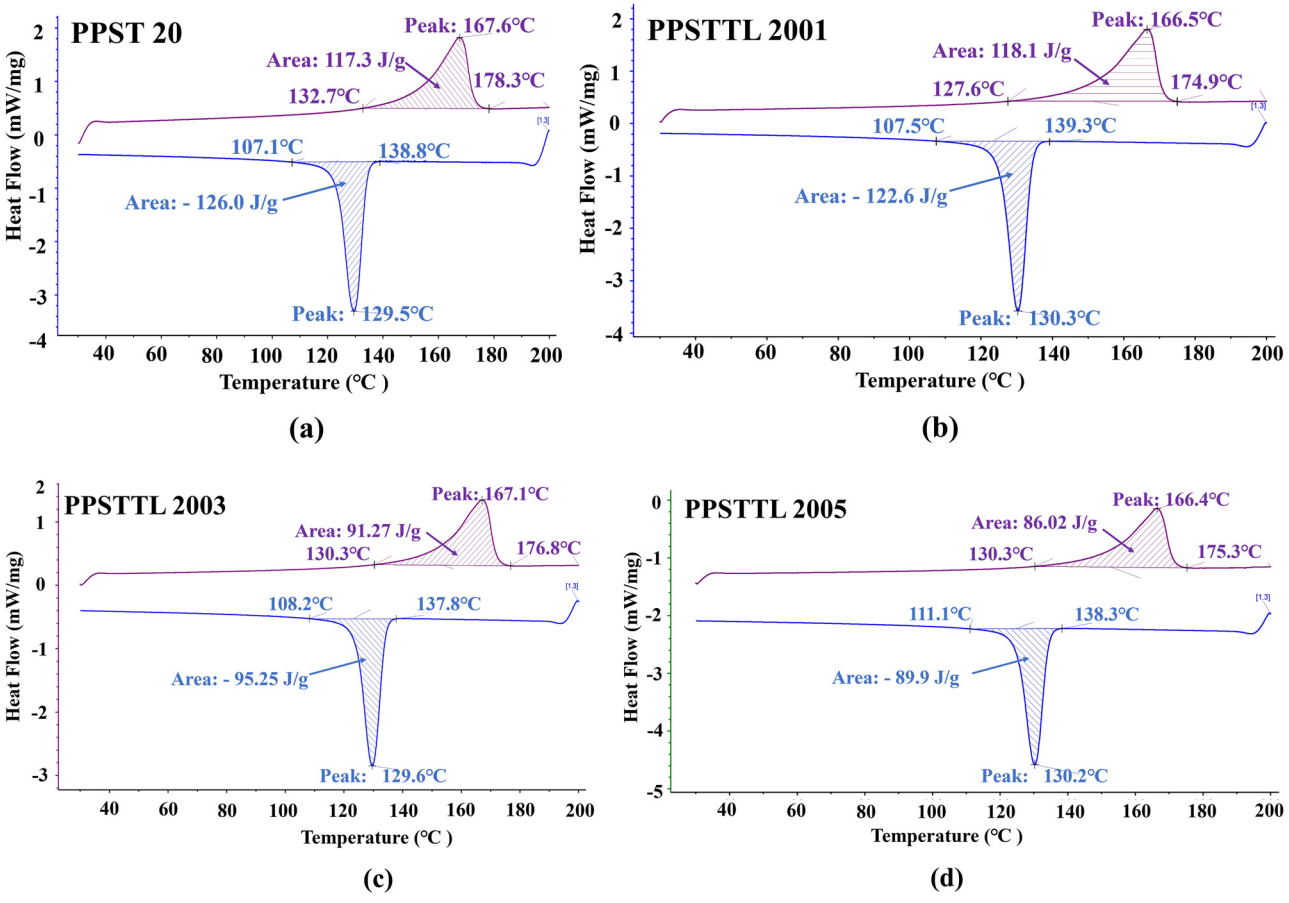

Figure 5: DSC thermogram of (a) PPST-20, (b) PPSTTL 2001, (c) PPSTTL 2003, and (d) PPSTTL 2005.

Table 4: DSC detailed data of PPST-20, PPSTTL 2001, 2003, and 2005

Samples	Melting temperature T_m (°C)	Enthalpy change ΔH_m (J/g)	Crystallization temperature T_c (°C)	Enthalpy change ΔH_c (J/g)	Degree of crystallinity X_c (%)
Pure PP	164.2	79.69	118.4	85.18	44.83
PPST-20	167.6	117.3	129.5	126	66.32
PPSTTL 2001	166.5	118.1	130.3	122.6	64.53
PPSTTL 2003	167.1	91.27	129.6	95.25	50.13
PPSTTL 2005	166.4	86.02	130.2	89.9	47.36

DSC thermogram and its summary in Table 3 reveal that PPST-20 exhibited the highest melting temperature and enthalpy of 167.6°C and 117.3 J/g, but the lowest crystallization temperature of 129.5°C when compared to pure PP, PPST-15, and PPST-25. This is indicative of enhanced processibility and improved mechanical and thermal stability offered by PPST-20. The higher melting temperature of PPST-20 indicates a higher degree of crystallinity in PPST-20, which is indicative of the presence of starch as an additive in the PP matrix. The area under the melting peak was found to be highest in PPST-20; this is indicative of increased heat of fusion, which can directly be related to the contribution of starch as an additive in increasing the crystallinity of bio-composite. Another DSC thermogram in Figure 5(a)–(d) represents the thermal behavior of PPST-20, PPSTTL 2001, 2003, and 2005 while being in the heating and cooling cycle. Data obtained from the thermogram are summarized in Table 4.

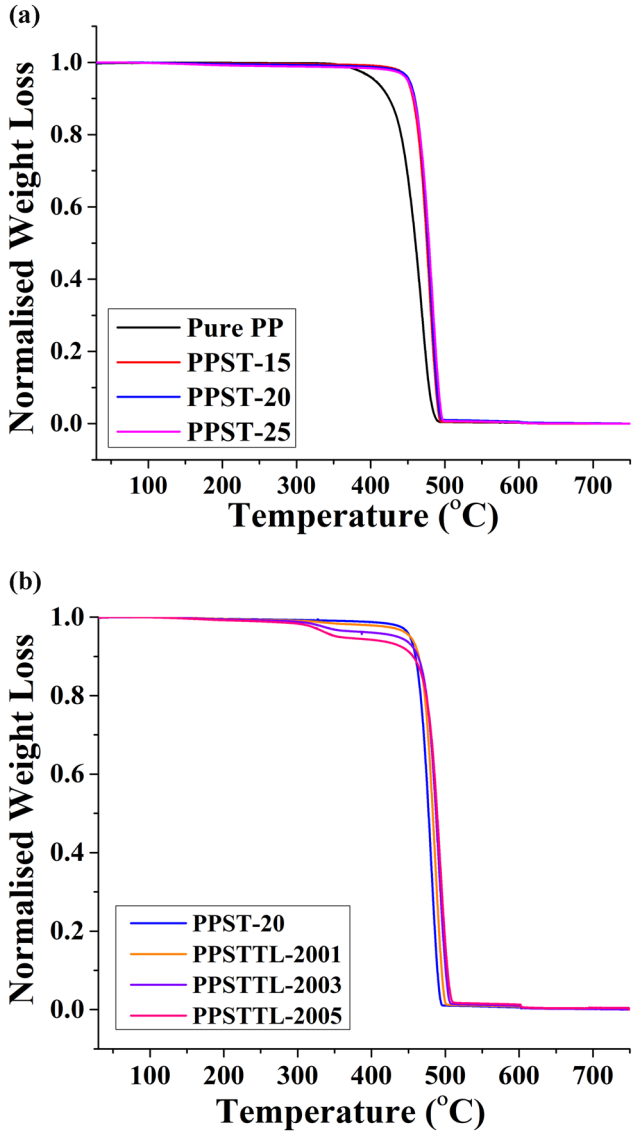

Figure 6: (a) TGA thermogram of pure PP, PPST-15, 20, and 25. (b) TGA thermogram of PPST-20, PPSTTL 2001, 2003, and 2005.

DSC thermogram and its summary in Table 4 reveal that PPSTTL 2003 exhibited the highest T_m among the other bio-nanocomposites, but the same was almost equal to that of PPST-20; however, a significant reduction in the enthalpy of PPSTTL 2003 and 2005 was found when compared to PPST-20 and PPSTTL 2001. Reduction in enthalpy can be attributable to the action of de-laminated nano-talc as a nucleating agent which increased the crystallization rate upon its infusion as nano-filler in PPST-20. Lowering of enthalpy in PPSTTL 2003 and 2005 indicates an increase in thermal stability, and it can lead to better dimensional stability and better stiffness of products developed by these polymeric bio-nanocomposites. The melting and crystallization behavior of bio-composite PPST-20 and bio-nanocomposite PPSTTL 2003 indicates that thermoplastic starch when acting alone in the PP matrix was serving the purpose of filler; however, infusion of delaminated nano-talc as a nucleating agent in the PP matrix improved the crystallization rate, thus reducing the total energy absorbed by the bio-nanocomposite.

4.5 TGA studies

During TGA testing, samples were heated from 30 to 750°C in the presence of nitrogen; TGA thermogram of the pure PP, PPST-15, 20, and 25 and PPST-20, PPSTTL 2001, 2003, and

Table 5: Decomposition temperature at 10, 50, and 75% weight loss

Samples	Td (°C) (10% weight loss)	Td (°C) (50% weight loss)	Td (°C) (75% weight loss)	Td (°C) (80% weight loss)
Pure PP	416.21	451.44	462.48	464.49
PPST-15	445.45	464.9	473.64	476.2
PPST-20	447.94	466.8	476.46	480.25
PPST-25	448.17	469.48	480.83	79% at 753.67
PPSTTL 2001	453.7	473.08	483.03	486.83
PPSTTL 2003	454.46	478.09	490.29	78% at 752.73
PPSTTL 2005	449.7	479.23	490.74	495.95

2005 was obtained and is presented in Figure 6(a) and (b), respectively, and data from the thermogram are summarized in Tables 5 and 6.

TGA thermogram and the corresponding summary table reveal that the bio-nanocomposite lost its moisture content between 30 and 200°C. Pure PP lost 10% of its weight around 416°C, whereas starch filling increased this temperature to 445–448°C for bio-composite, which was further elevated between 449 and 453 upon the addition of delaminated nano-talc. PP usually loses its significant weight above 300°C, this was verified by 90% weight loss of pure PP at 500°C, but a significant decrease in % decomposition (78–85% for bio-composite and 68–80% for bio-nanocomposite) at this temperature was observed considering the fusion of thermoplastic starch and nano-talc in it. TGA studies reveal the enhanced ability to sustain thermal stress to a great extent by the addition of nano-talc in the PPST-20.

4.6 Tensile strength and % elongation

Tensile strength and elongation of pure-PP and its bio-composite PPST-15, 20, and 25 and bio-nanocomposite PPSTTL 2001, 2003, and 2005 were evaluated and presented as a bar graph in Figure 7(a) and (b), respectively.

The bar graph reveals the tensile strength of PPSTTL 2003 and PPST-20 to be 28.32 and 29.27 MPa, respectively, which is comparable to that of 30.72 MPa of pure PP. As far as % elongation of bio-nanocomposite is concerned, a significant decrease was observed in all the specimens; however,

Table 6: Decomposition at 30–200, 600, and 750°C

Samples	% decomposition of samples		
	30–200°C	500°C	750°C
Pure PP	0.163	99.70	0
PPST-15	0.224	85.72	0.27
PPST-20	0.253	80.96	0.453
PPST-25	0.679	78.65	0.284
PPSTTL 2001	0.392	80.20	0.617
PPSTTL 2003	0.36	69.80	0.734
PPSTTL 2005	0.664	68.00	0.842

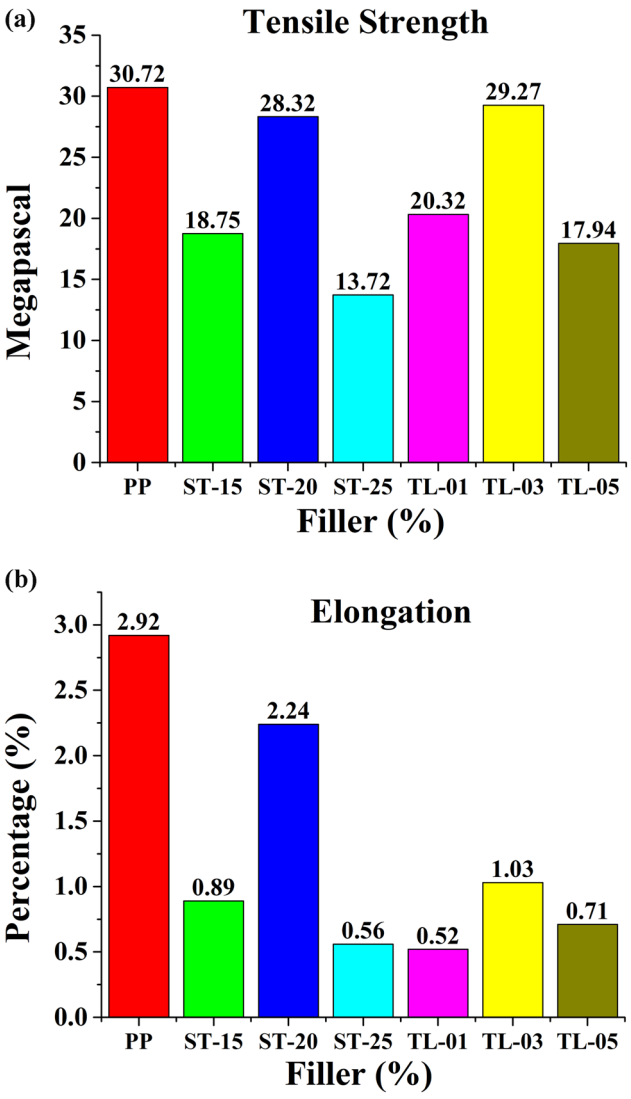

Figure 7: (a) Tensile strength of pure PP, bio-composite, and bio-nanocomposite. (b) % elongation of pure PP, bio-composite, and bio-nanocomposite.

PPSTTL 2003 and PPST-20 exhibited the lowest decrease in elongation, *i.e.*, 1.03 and 2.24%, respectively, and the same was confirmed by the DSC studies also. A higher value of tensile strength of PPSTTL 2003 and PPST-20, but the reduction in the % elongation can be attributable to the high crystalline nature and faster crystallization behavior of materials as is verified in the thermal and XRD studies.

4.7 Flexural properties

Flexural strength and flexural modulus of the pure PP and its bio-composite PPST-15, 20, and 25 and bio-nanocomposite PPSTTL 2001, 2003, and 2005 are presented as bar graphs in Figure 8(a) and (b), respectively.

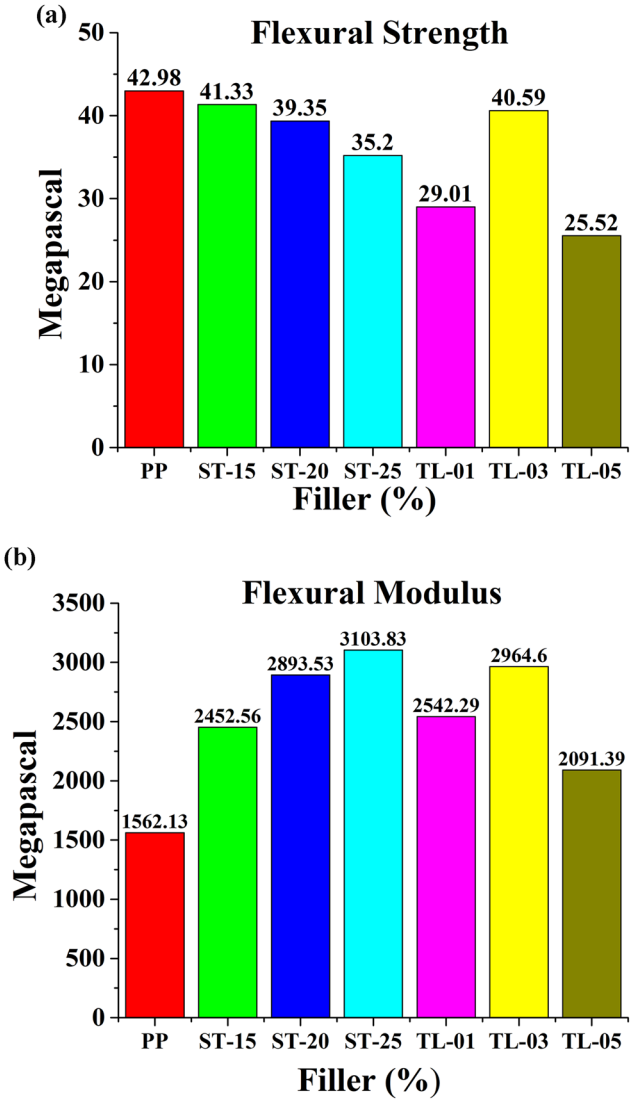

Figure 8: (a) Flexural strength of pure PP, bio-composite, and bio-nanocomposite. (b) Flexural modulus of the pure PP, bio-composite, and bio-nanocomposite.

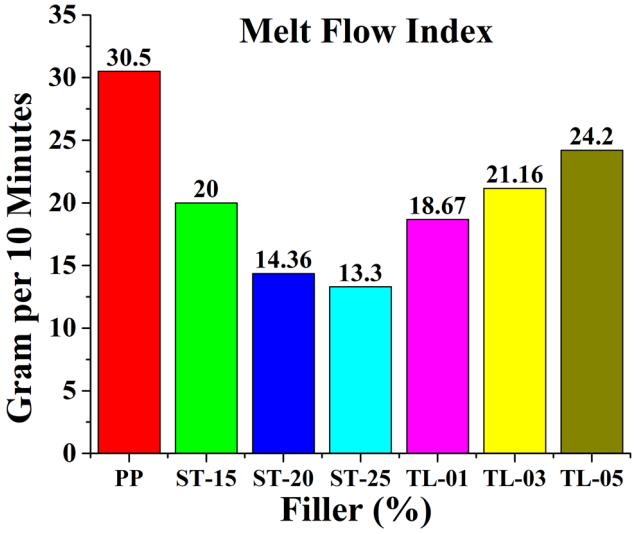

Figure 9: MFI of pure PP, bio-composite, and bio-nanocomposite.

The bar graph reveals an expected decrease in the flexural strength but an increase in the flexural modulus of bio and bio-nanocomposite. The decrease in flexural strength of bio and bio-nanocomposite can be attributable to the poor interface and hydrophilic nature of starch; however, talc content of 3% in PPSTTL 2003 seems to have induced higher flexural strength and flexural modulus, attributable only to its function as nucleating agent. Here, de-laminated talc acts as the nucleating center, which was confirmed by the DSC studies also; this is further verified by a reduction in the enthalpy of the bio-nanocomposites. Thus, bio-nanocomposites developed in this study exhibit better processibility, enhanced mechanical properties, better thermal stability, and very good dimensional stability.

4.8 Melt flow properties

The MFI of the pure PP and its bio-composite PPST-15, 20, and 25 and bio-nanocomposite PPSTTL 2001, 2003, and 2005 are presented as bar graphs in Figure 9.

The bar graph revealed almost linear decreases in the MFI of starch-based bio-composite upon increasing starch content; this is in line with the expected starch behavior due to its poor interface and hydrophilic nature, but, infusion of de-laminated nano-talc in PPST-20 increased its MFI due to its nucleating action. Infusion of talc in the PPST-20 increased the processability of bio-composite, thus making it more suitable for industrial processability. Results indicate that bio-filled nanocomposites when compared with

inorganic fillers induce reduced friction in the machine, thus increasing the life cycle of the screw and barrel of the twin-screw extruder.

5 Conclusion

In this research work, thermoplastic potato starch and delaminated nano-talc-based sustainable bio-nanocomposite of PP were prepared first time by ultra-high-speed melt thermo-kinetic mixing method. Spectral, mechanical, thermal, and optical properties of the bio-nanocomposite were studied for the optimal bio- and nanofillers. At first, the concentration of thermoplastic starch in the PP matrix was kept at 15, 20, and 25%, among which 20% starch content yielded tensile strength, elongation, flexural strength, MFI, and a melting point of 28.32 MPa, 2.24%, 43.35 MPa, 14.36 g/10 min, and 167.6°C, respectively, which was comparatively better than other formulations. In the second stage, the concentration of starch in the PP matrix was kept at 20% while talc as nano-filler was varied to 1, 3, and 5% and characterized by FTIR and XRD spectroscopy. This confirmed the crystal size of starch and nano-talc molecules in bio-nanocomposite, and its uniform dispersion in the PP matrix. Larger *d*-spacing was found in all the bio-composites when compared to the pure PP, which suggested loose packing and disoriented starch molecules within the crystalline structure. Reduction in the *d*-spacing was also found upon the addition of nano-talc in the bio-composite with 20% starch concentration, which confirmed the nucleating action of talc molecules, thus lowering their *d*-space. This is indicative of close packaging and more orderly distribution of nanoparticles within the PP matrix. XRD results also indicated disorientation of the starch molecules, whereas UV–Vis studies indicated its photosensitizer properties, which were responsible for the increased UV absorbance by the bio-composite materials. This effect was counterpoised by the nucleating effect of nano-talc in the bio-nanocomposite (PPSTTL 2003 and 2003) with 3 and 5% nano-talc concentrations. DSC and TGA studies revealed an increase in thermal stability and lowering of the enthalpy which ultimately led to the improvement in the thermal behavior of the bio-nanocomposite when exposed to elevated thermal stress for a longer duration. Lowering of enthalpy can also be attributable to the corresponding change in its mechanical properties. Flexural properties of the bio-nanocomposite were found to be comparable to pure PP but melt flow studies indicated a slight decrease in processability linked to an increase in starch content; this was reversed to a large extent upon incorporation of nanomaterial. Finally, we can conclude by summarizing the encouraging results indicating the successful incorporation of 20% bio-material and 3% nanomaterial in PP for lightweight and high-performance bio-nanocomposite materials with low enthalpy for structural components to be used in several advanced applications, *i.e.*, aerospace, automotive, energy storage, biomedical devices, advanced battery separators, and electrolytes.

Acknowledgments: Spectral testing, such as FTIR spectroscopy for the constituent polymer identification, UV–Vis spectroscopy for optical absorbance spectrum, and X-ray diffraction tests, was done at University Instrumentation Centre (UIC), Manav Rachna University, Faridabad, Haryana, India. All the tests were done as per applicable ISO and ASTM standards.

Funding information: Authors state no funding involved.

Author contributions: All the authors jointly designed the experiments; Rakesh Goswami and Aftab Alam performed the experimentation and interpretation of experimental data. Rakesh Goswami prepared the manuscript with contributions from all the co-authors. All authors have accepted responsibility for the entire content of this manuscript and approved its submission.

Conflict of interest: Authors state no conflict of interest.

Data Availability Statement: All data generated or analysed during this study are included in this published article.

References

[1] Iskalieva A, Orazalin Zh, Yeligayeva G, Irmukhametova G, Taburova S, Tokter T. Synthesis of biodegradable polymer-based on starch for packaging films: A review. Complex Use Miner Resourcs. 2024;329(2):110–30. doi: 10.31643/2024/6445.20.

[2] Ghasemi AF, Ghasemi I, Menbari S, Ayaz M, Ashori A. Optimization of mechanical properties of polypropylene/talc/graphene composites using response surface methodology. Polym Test. 2016;53:283–92. doi: 10.1016/j.polymertesting.2016.06.012.

[3] Liu W, Wang YJ, Sun Z. Crystallization behavior of starch-filled polypropylene. J Appl Polym Sci. 2004;92(1):484–92. doi: 10.1002/app.20019.

[4] Szeberényi A, Adam BY, Sharma H, Dhivya A. Plastic recycling & waste management. 1st edn. India: JSR Publications; 2023.

[5] McGlinchey S, Walters R, Scheinpflug C, eds. International Relations Theory. 1st edn. Bristol, England: E-International Relations Publishing; 2017.

[6] Bos P, Ritzen L, Dam SV, Balkenende R, Bakker C. Bio-based plastics in product design: The state of the art and challenges to overcome. Sustainability. 2024;16(8):3295. doi: 10.3390/su16083295.

[7] Reddy MM, Vivekanandhan S, Misra M, Bhatia SK, Mohanty A. Biobased plastics and bionanocomposites: Current status and future opportunities. Prog Polym Sci. 2013;38(10–11):1653–89. doi: 10.1016/j.progpolymsci.2013.05.006.
[8] Hietala M, Mathew AP, Oksman K. Bionanocomposites of thermoplastic starch and cellulose nanofibers manufactured using twin-screw extrusion. Eur Polym J. 2013;49(4):950–6. doi: 10.1016/j.eurpolymj.2012.10.016.
[9] Corrêa AC, Teixeira EM, Pessan LA, Mattoso LHC. Cellulose nanofibers from curaua fibers. Cellulose. 2010;17(6):1183–92. doi: 10.1007/s10570-010-9453-3.
[10] Rahmat AR, Rahman WAWA, Sin LT, Yussuf AA. Approaches to improve compatibility of starch filled polymer system: A review. Mater Sci Eng C. 2009;29(8):2370–7. doi: 10.1016/j.msec.2009.06.009.
[11] Zhang S, He Y, Yin Y, Jiang G. Fabrication of innovative thermoplastic starch bio-elastomer to achieve high toughness poly(butylene succinate) composites. Carbohydr Polym. 2019;206:827–36. doi: 10.1016/j.carbpol.2018.11.036.
[12] Ilyas RA, Sapuan SM. The preparation methods and processing of natural fibre bio-polymer composites. Curr Org Synth. 2019;16(8):1068–70. doi: 10.2174/1570179416082001201056l6.
[13] Skoczinski P, Carus M, Tweddle G, Ruiz P, de Guzman D, Ravenstijn J, et al. Bio-based building blocks and polymers – Global capacities, production and trends 2022–2027. Hürth, Germany: Nova-Institute GmbH Leyboldstr; 2023 Feb. [cited 2024 Aug 26] doi: 10.52548/CMZD8323.
[14] Obasi HC, Egeolu FC, Ezenwajiaku HI. Effect of starch content and compatibilizer on the mechanical, water absorbance and biodegradable properties of potato starch filled propylene blends. Quantum J Environ Stud. 2019;1(1):32–43. https://myjms.mohe.gov.my/index.php/qjoes/article/view/8265.
[15] Karthikeyan R, Shilaja C, Sivalingam A, Gopinath P. Experimental investigations on mechanical and water absorption properties of epoxy resin-banana fiber-tamarind seed particles hybrid biocomposites. Mater Today: Proc. 2022;68(6):2220–5. doi: 10.1016/j.matpr.2022.08.436.
[16] Roy SB, Shit SC, Sengupta RA, Shukla PR. Biodegradability studies of bio-composites of polypropylene reinforced by potato starch. Int J Innov Res Sci Eng Technol. 2015;4(3):1120–30. doi: 10.15680/IJIRSET.2015.0403066.
[17] Adetunji CO, Olotu T, Mathew JT, Abel I, Olugbemi TO, Adetunji MC, et al., eds. Chapter 18: Morphology, rheology, properties, and applications of nanostarch-filled polymer blends. In Thomas S, George SC, Nair ST, editors. Micro and Nano Technologies, Nanofiller for binary blends. Elsevier; 2024. p. 443–64. doi: 10.1016/B978-0-323-88655-0.00005-7.
[18] Chandramouleeswaran S, Mhaske ST, Kathe AA, Varadarajan PV, Prasad V, Vigneshwaran N. Functional behaviour of polypropylene/ZnO-soluble starch nanocomposites. Nanotechnology. 2007;18(38):385702. doi: 10.1088/0957-4484/18/38/385702.
[19] Roy SB, Ramaraj B, Shit SC, Nayak SK. Polypropylene and potato starch biocomposites: Physicomechanical and thermal properties. J Appl Polym Sci. 2011;120(5):3078–86. doi: 10.1002/app.33486.
[20] Morán JI, Vázquez A, Cyras VP. Bio-nanocomposites based on derivatized potato starch and cellulose, preparation and characterization. J Mater Sci. 2013;48(20):7196–203. doi: 10.1007/s10853-013-7536-x.
[21] Ilyas RA, Sapuan SM, Ibrahim R, Abral H, Ishak MR, Zainudin ES, et al. Thermal, biodegradability and water barrier properties of bio-nanocomposites based on plasticised sugar palm starch and nanofibrillated celluloses from sugar palm fibres. J Biobased Mater Bioenergy. 2020;14(2):1–13. doi: 10.1166/jbmb.2020.1951.
[22] Ilyas RA, Sapuan SM, Atiqah A, Ibrahim R, Abral H, Ishak MR, et al. Sugar palm (Arenga pinnata [Wurmb.] Merr) starch films containing sugar palm nanofibrillated cellulose as reinforcement: Water barrier properties. Polym Compos. 2019;41(2):459–67. doi: 10.1002/pc.25379.
[23] Peregrino PP, Sales MJA, Silva MFP, Soler MAG, DaSilva LFL, Moreira SGC, et al. Thermal and electrical properties of starch-graphene oxide nanocomposites improved by photochemical treatment. Carbohydr Polym. 2014;106(1):305–11. doi: 10.1016/j.carbpol.2014.02.008.
[24] Kaseem M, Hamad K, Deri F. Rheological and mechanical properties of polypropylene/thermoplastic starch blend. Polym Bull. 2012;68(4):1079–91. doi: 10.1007/s00289-011-0611-z.
[25] Oduola MK, Akpeji PO. Effect of starch on the mechanical and rheological properties of polypropylene. Am J Chem Eng. 2015;3(2–1):1–8. doi: 10.11648/j.ajche.s.2015030201.11.
[26] Ammar O, Bouaziz Y, Hadar N, Minaf N. Talc as reinforcing filler in polypropylene compounds: Effect on morphology and mechanical properties. Polym Sci. 2017;3(2):1–7. doi: 10.4172/2471-9935.100023.
[27] Leong WY, Ishak ZAM, Ariffin A. Mechanical and thermal properties of talc and calcium carbonate filled polypropylene hybrid composites. J Appl Polym Sci. 2004;91(5):3327–36. doi: 10.1002/app.13543.
[28] Karsli NG, Aytac A. Effects of maleated polypropylene on the morphology, thermal and mechanical properties of short carbon fiber reinforced polypropylene composites. Mater Des. 2011;32(7):4069–73. doi: 10.1016/j.matdes.2011.03.021.
[29] Thabet A, Mobarak Y. Predictable models and experimental measurements for electric properties of polypropylene nanocomposite films. Int J Elect Comp Eng. 2016;6(1):120–9. doi: 10.11591/ijece.v6i1.9108.
[30] Anozie OO, Dilibe Ifeanyi ND. Mathematical modelling of mechanical properties polypropylene/talc composites: Power equation approach. Int J Res Adv Eng Technol. 2016;2(4):15–9. https://www.allengineeringjournal.in/assets/archives/2016/vol2issue4/2-5-12-490.pdf.
[31] Lapcik L, Jindrova P, Lapcikova B, Tamblyn R, Greenwood R, Rowson N. Effect of the talc filler content on the mechanical properties of polypropylene composites. J Appl Polym Sci. 2008;110(5):2742–7. doi: 10.1002/app.28797.
[32] Zihlif AM, Ragosta G. Mechanical properties of talc-polypropylene composites. Mater Lett. 1991;11(10–12):368–72. doi: 10.1016/0167-577X(91)90136-T.
[33] Wu G, Wen B, Hou S. Preparation and structural study of polypropylene-talc gradient materials. Polym Int. 2004;53(6):749–55. doi: 10.1002/PI.1360.
[34] Järvelä PA, Enqvist J, Järvelä PK, Tervala O. Mechanical strength and thermal stability of magnesium silicate filled polypropylenes [Internet]. Compos Interfaces. 2001;8(3–4):189–206. doi: 10.1163/15685540152594668.
[35] Jeziorska R, Szadkowska A, Studzinski M, Chmielarek M, Spasowka E. Morphology and selected properties of modified potato thermoplastic starch. Polymers. 2023;15(7):1762. doi: 10.3390/polym15071762.
[36] Paluch M, Ostrowska J, Tyński P, Sadurski W, Konkol M. Structural and thermal properties of starch plasticized with glycerol/urea mixture. J Polym Env. 2022;30(2):728–40. doi: 10.1007/s10924-021-02235-x.

[37] Meligi GA, El-Rehim HAA, Hegazy ESA, Rabie AM. Degradation of polypropylene and polyprop/starch blends. Polym & Polym Compos. 2009;17(4):265–72. doi: 10.1177/096739110901700405.
[38] Li X, Zhang Y, He Y. Rapid detection of talcum powder in tea using FT-IR spectroscopy coupled with chemometrics. Sci Rep. 2016;6:30313. doi: 10.1038/srep30313.
[39] Wu H, He M, Wu S, Yang M, Liu X. Near-infrared spectroscopy study of OH stretching modes in pyrophyllite and talc. Crystals. 2022;12(12):1759. doi: 10.3390/cryst12121759.
[40] Liu X, Liu X, Hu Y. Investigation of the thermal decomposition of talc. Clays Clay Min. 2014;62(2):137–44. doi: 10.1346/CCMN.2014.0620206.
[41] Lee D, Kim S, Kim BJ, Chun SJ, Lee SY, Wu Q. Effect of Nano-$CaCO_3$ and talc on property and weathering performance of PP composites. Int J Polym Sci. 2017;2017(2):1–9. doi: 10.1155/2017/4512378.
[42] Liu K, Stadlbauer W, Zitzenbacher G, Paulik C, Burgstaller C. Effects of surface modification of talc on mechanical properties of polypropylene/talc composites. AIP Conf Proc. 2016;1713:120008. doi: 10.1063/1.4942323.